

Synthesis and characterization of zinc gallate based compounds for luminescence

A Dissertation Report for
Course code and Title: PHGO-313 Dissertation
Credits: 8
Submitted in partial fulfilment of Master's Degree
M.Sc. in Physics/Solid State Physics

by

SAMUEL D'SOUZA

Roll Number: 21P043010

VICTOR D'SOUZA

Roll Number: 21P043011

Under the Supervision of

DR. SUDHIR CHERUKULAPPURATH

School of Physical and Applied Science
Physics



GOA UNIVERSITY

DATE: MAY 2023



Examined by:

[Handwritten signatures of examiners]

Seal of the School

DECLARATION BY STUDENT

We hereby declare that the work presented in this Dissertation entitled "Synthesis and Characterisation of Zinc Based Compounds for Luminescence" is based on the results of investigations carried out by us in Physics at the School of Physical and Applied Science, Goa University under the Supervision Dr. Sudhir Cherukulappurath and the same has not been submitted elsewhere for the award of a degree or diploma by us. Further, we understand that Goa University or its authorities will be not be responsible for the correctness of observations / experimental or other findings given the dissertation.

I hereby authorize the University authorities to upload this dissertation on the dissertation repository or anywhere else as the UGC regulations demand and make it available to any one as needed.



Mr. Samuel D'souza

21P043010

Physics

School of Physical and Applied Science



Mr. Victor D'souza

21P043011

Physics

School of Physical and Applied Science

Date:

Place: Goa University

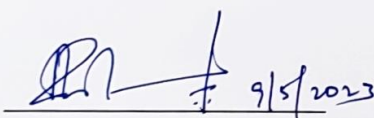
COMPLETION CERTIFICATE

This is to certify that the dissertation "**Synthesis and Characterization of Zinc Gallate Based Compounds for Luminescence**" is a bonafide work carried out **Mr. Samuel D'souza and Mr. Victor Dsouza** under my supervision in partial fulfilment of the requirements for the award of the degree of **Master's** in the Discipline Physics at the School of Physical and Applied Sciences, Goa University.



Dr. Sudhir Cherukulappurath
Physics

Date:



Prof. Kaustubh R.S. Priolkar
Physics
School of Physical and Applied Sciences

Date:

Place: Goa University



School Stamp

ACKNOWLEDGEMENT

We would like to express our deepest gratitude to our guide, Dr. Sudhir Cherukulappurath for his guidance, encouragement, and immense knowledge.

We would also like to appreciate Dr. Kaustubh R.S Priolkar (Head of Department) for his support and for the knowledge imparted.

We are very grateful to Ms. Namita Rane for her help, guidance, and constant motivation throughout our dissertation work.

We acknowledge the support and express our profound gratitude to our friends and family.

The completion of this dissertation would not be possible without them.

ABSTRACT

Nanoparticles have gained interest in recent years with many applications in bio-imaging with ex-vivo excitation. This is because of their remarkable optical and luminescent properties which permit UV excitation and delayed emission. Through this dissertation we present our work on the preparation of one of these type of nanoparticles:- Zinc Gallate. A hydrothermal synthesis was used to prepare undoped zinc gallate. The sample was successfully doped with transition metals such as manganese, chromium, cobalt, and nickel using the sample synthesis. The optical and luminescent properties were studied by various characterisation methods. The X-ray Diffraction analysis showed that the samples prepared had an average crystallite size of 12.28nm. Scanning electron microscopy gave an average particle size in the nanometre range. UV Visible spectroscopy was used to find the band gap of the prepared materials. Each sample had a different band gap but in the range of 4.3eV to 4.8eV. The average band gap was found to be 4.7eV. Using photoluminescent spectroscopy we obtained the emission spectrum and concluded the presence of two major peaks corresponding to the R-phonon line due to the d-d transition from ${}^2E - {}^4A_2$ and the N_2 band due to the Cr^{+3} ions which are distorted by the antisite defect.

LIST OF FIGURES

1. Cubic spinel structure of ZGO [1]
2. Simplified Jablonski diagram representing different relaxation pathways following absorption of a UV photon
3. Persistent Luminescence decay curve and NIR images at different afterglow times [5]
4. Energy level diagram of Cr³⁺ ion in the octahedral crystal field [2]
5. Schematic of the NIR Persistent Luminescence mechanism; 1–7 represent electron-transfer processes in ZGC [2]
6. The energy diagram of Cr³⁺ in the octahedral symmetry [3]
7. Chemical reaction to show the formation of zinc gallate [3]
8. Diffraction of Xray beam through a crystal
9. XRD pattern of zinc gallate and Cr, Ni, Co, and Mn doped Zinc Gallates before annealing.
10. XRD pattern of zinc gallate and Cr, Ni, Co, and Mn doped Zinc Gallates after annealing.
11. SEM images of 1) Ni annealed, 2) Annealed Undoped, 3) Annealed Cr doped, 4) Cr doped, 5) Undoped, 6) Ni doped Zinc gallate.
12. Absorption spectra and tauc plot for samples before annealing.
13. Absorption spectra and tauc plot for samples after annealing.
14. a) Emission Spectrum of ZGC at $\lambda_{ex}=254\text{nm}$, Phosphorescence decay at b)686nm shows as average lifetime of 112.59 μs and c)695nm shows an average lifetime of 112.70 μs .

15. a) Emission Spectrum of ZGC at $\lambda_{\text{ex}}=400\text{nm}$, Phosphorescence decay at b)686nm shows as average lifetime of 112.29 μs and c)696nm shows an average lifetime of 113.07 μs .

16. a) Emission Spectrum of ZGC at $\lambda_{\text{ex}}=532\text{nm}$, Phosphorescence decay at b)686nm shows as average lifetime of 112.23 μs and c)696nm shows an average lifetime of 110.52 μs .

LIST OF TABLES

1. The crystal sizes of Cr-ZGO prepared under different pH environments and different base addition rates [3]
2. List of chemicals
3. Calculation for preparation of zinc gallate
4. Calculation for preparation of Cr doped zinc gallate
5. Calculation for preparation of Ni doped zinc gallate
6. Calculation for preparation of Co doped zinc gallate
7. Calculation for preparation of Mn doped zinc gallate
8. Crystallite size, interplanar distance and lattice parameter, before and after annealing.
9. The change in band gap before and after annealing.

INDEX

Title	Page No.
Chapter 1: Brief Overview	11-14
1. Introduction	12
1.1. Objectives	12
1.2. Zinc Gallate	12
1.3. Nanomaterials	13
1.4. Synthesis and Characterization	14
Chapter 2 Luminescent Properties	15-26
2. Luminescence	16
2.1. Photoluminescence	16
2.1.1. Fluorescence and Phosphorescence	16
2.2. Persistent Luminescence	18
2.3. Mechanisms	20
2.3.1. Crystal Field Splitting	20
2.3.2. Persistent Luminescent Mechanism	21
2.3.3. Octahedral Symmetry of Cr ⁺³	22
2.4. Factors affecting luminescence	23
2.4.1. Nature and composition of dopant	23
2.4.2. Effect of pH	24
2.4.3. Annealing Temperature	25
2.4.4. Effect of Excitation Wavelength	26
Chapter 3: Synthesis	27-34
3. Synthesis	28

3.1. Methods of Synthesis	28
3.1.1. Sol-Gel Method	28
3.1.2. Hydrothermal Method	29
3.2. Sample Preparation	30
3.2.1. List of Chemicals	30
3.2.2. Calculation for respective sample preparations	31
3.2.3. Procedure	33
Chapter 4: Characterization & Results	35-46
4. Results	36
4.1. Xray Diffraction	36
4.2. Scanning Electron Microscopy	39
4.3. UV Visible Spectroscopy	41
4.4. Photoluminescent Spectroscopy	43
Chapter 5: Conclusion	47-49
5.1 Applications	48
5.2 Conclusion	48
Bibliography	50-52

Chapter 1:

Brief Overview

1. Introduction

1.1. Objectives

- Synthesize zinc gallate nanoparticles
- Synthesize Cr, Mn, Co, and Ni-doped zinc gallate nanoparticles
- Determine the particle size using scanning electron microscopy
- Verify and determine crystallite size using x-ray diffraction
- Determine optical band gap using UV-Visible spectroscopy
- Study the photoluminescence spectrum of the prepared samples
- Verify persistent luminescent properties of the prepared sample

1.2. Zinc Gallate (ZnGa_2O_4)

Zinc gallate (ZnGa_2O_4) is a p-type semiconductor with a large band gap (4.4-5.2 eV). It is a double oxide phosphor and is a promising phosphor because of its chemical and thermal stability and blue emission when irradiated by UV light. It has a lattice parameter of 8.334 Å and crystallizes into a normal cubic AB_2O_4 spinel crystal. Zn^{2+} ions occupy the A sites with tetrahedral coordination while Ga^{3+} ions occupy the B sites with octahedral coordination. These sites are surrounded by 4 and 6 oxygen ions respectively.

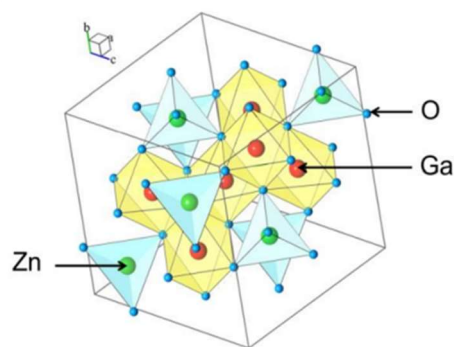


Figure 1: Cubic spinel structure of ZGO [1]

It exhibits a slight inversion character, wherein a few percent of Zn^{+2} ions occupy B sites while a few percent of Ga^{+3} ions occupy A sites. Such defects in the host matrix are called antisite defects. It was noted that $ZnGa_2O_4$ exhibits about 3% inversion. It is worth mentioning that the fraction of defects depends on the preparation method, annealing temperature, and/or dopant content. This however is a conclusion drawn from the literature review.

The emission spectrum of zinc gallate can be tuned by doping with rare-earth or transition-metal ions. A good example is Cr^{3+} whose ionic radius is 0.64 \AA while that of Ga^{3+} is 0.62 \AA . It is important that their ionic radii are similar. This enables Cr^{3+} to effectively substitute Ga^{3+} ions in the spinel structure. $ZnGa_2O_4$ doped with Cr^{3+} ions exhibit a bright emission in the red-to-near-infrared (NIR) region, i.e., 800-2500nm. Long-lasting phosphorescence or persistent luminescence arises in $ZnGa_2O_4$ doped with chromium because of the Cr^{+3} distortion by a neighbouring antisite defect.

Zinc gallate nanocrystals find applications in bioimaging. Their size can be tuned to be comparable in size to the biomolecules they are labelling to not interfere with cellular systems.

1.3 Nanomaterials

Nanomaterials are materials with at least one external dimension that measures 100 nanometres (nm) or less or with internal structures measuring 100 nm or less. The nanomaterials that have the same composition as known materials in bulk form, may have different physio-chemical properties.

The term nanoscale refers to the dimensions of 10^{-9} metres, which is a billionth part of a metre. Nanomaterials can be of many types. They are called nanoparticles when all 3 dimensions are within the nanoscale range and are called nanofibers if only 2

dimensions are such. Nanomaterials can exist as nanotubes, which are hollow nanofibers, or nanorods, which are solid nanofibers.

Nanomaterials can be synthesized by 2 approaches, top-down approach, or bottom-up approach.

For the preparation of zinc gallate nanoparticles we have chosen the bottom-up approach.

1.4 Synthesis and Characterization

We synthesized zinc gallate using the hydrothermal process using zinc nitrate and gallium nitrate as precursors. Using the same synthesis, we successfully doped zinc gallate with manganese, chromium, cobalt, and nickel. The samples were annealed at 800°C. The crystallinity and purity of the sample were determined by means of X-ray diffraction. The average crystallite size and the lattice constants were also calculated using the data obtained. Scanning electron microscopy provided magnified images as well as approximate particle size. UV visible Spectroscopy was performed to calculate the band gap and observe the excitation curve. Further photoluminescent and persistent luminescent studies were carried out to observe prominent peaks.

CHAPTER 2: LUMINESCENT PROPERTIES

2. Luminescence

Luminescence is the property of a material to absorb incident radiation and re-emit it as light of lower energy. Such emissions occur when materials absorb energy from UV radiations or high-energy electron beams and jump to the excited state. De-excitation and emission of light are due to the instability of the excited state. A luminescent material emits “cold light” in contrast to incandescence, wherein an object only emits light after heating. Luminescence is a naturally occurring phenomenon. Fireflies, Aurora Borealis, etc. are good examples.

Every luminescent process contains two major processes; absorption/excitation and emission. Based on the source of excitation, luminescence can be classified into different types. When an electric current caused by an externally applied bias is used, we call the process electroluminescence. If electromagnetic radiation is used, it is called Photoluminescence.

2.1. Photoluminescence

Photoluminescence is one such type of luminescence wherein the electromagnetic radiation is used in the excitation process. It can further be classified into Fluorescence or Phosphorescence based on the time delay between excitation and emission.

2.1.1. Fluorescence & Phosphorescence

The process is fluorescent when the time delay is short, i.e., 10^{-8} - 10^{-4} s, and is phosphorescent when the time delay is longer. Eu^{2+} doped alkaline earth phosphors, alkaline silicate phosphors, zinc gallates doped with transition metal ions, etc. show long-lasting phosphorescence.

Atoms of different elements have different numbers of electrons in different energy levels. Every electron has a spin. Hence two electrons can interact with each other and either exists in the singlet state or the triplet state. The singlet state is formed when paired electrons have opposite spins. Hence the net spin is zero. The triplet state is formed when the electrons pair with parallel spins.

In the ground state, the molecular energies are constant and have a minimum value. When energy is supplied in the form of radiation, the molecule can absorb energy and transition from the ground state to a higher energy electronic state like S_1 (first electronic singlet state) or S_2 (second electronic singlet state). Such transitions are dependent on the type of molecule and the wavelength (energy) of the incident radiation.

The electrons remain in the excited singlet state for 10^{-8} - 10^{-4} s and then revert to the ground state with the emission of energy. This is called fluorescence. The emitted wavelength is longer than the incident wavelength. The electrons can assume a triplet state instead of transitioning to the ground state like in the previous case. The electrons then transition, after some time, to the ground state with the emission of energy in the form of light. This is called phosphorescence.

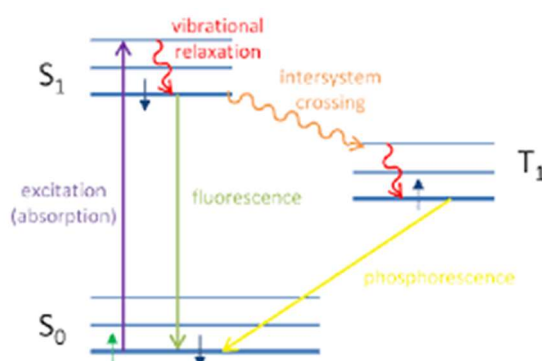


Figure 2: Simplified Jablonski diagram representing different relaxation pathways following absorption of a UV photon

Hence, fluorescence is the immediate emission of absorbed radiation while phosphorescence is the delayed emission of absorbed radiation. In both cases, the emitted light has a longer wavelength and lower energy as compared to the absorbed light because part of the energy is released by non-radiative decay processes. Hence UV excitations produce emissions in the visible region.

Zinc gallate is an excellent photoluminescence host material when doped with transition metals such as $\text{ZnGa}_2\text{O}_4: \text{Mn}^{+2}$ for green emission and $\text{ZnGa}_2\text{O}_4: \text{Cr}^{+3}$ for red or near-infrared emission.

2.2. Persistent Luminescence

Persistent Luminescence, also called afterglow/long-lasting phosphorescence, is a phenomenon in which luminescence can last for minutes and even hours after the stoppage of excitation. Afterglow or persistent luminescence materials can store energy from UV light, visible light, X-ray, or some other excitation sources and then gradually release it by a photonic emission.

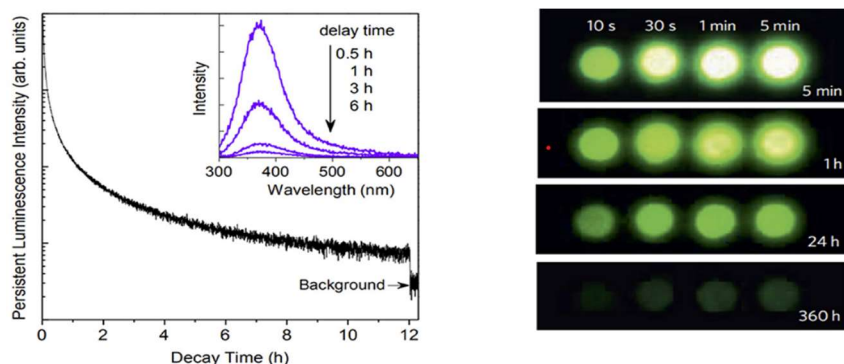


Figure 3: Persistent Luminescence decay curve and NIR images at different afterglow times.^[5]

The unique properties of persistent luminescence materials mainly come from two kinds of active centres involved: the emitter centres and the trap centres. The emitter centres can emit radiation after excitation. So, the emission wavelength of a persistent luminescence phosphor depends upon the emitter. The trap centres are formed due to impurities, lattice defects, or various co-dopants. They usually do not emit radiation, but store the excitation energy for some time and then gradually release it to the emitters. Therefore, the persistent intensity and time are mainly determined by the traps. In the design of persistent luminescence materials, a suitable emitter centre and a proper host that can create appropriate traps and release long-lasting persistent luminescence (PL) should be considered.

Shallow traps can be depopulated very fast at room temperature via the material's conduction band but this is not true for deeper traps. This differentiates it from phosphorescence which, as mentioned before, is a result of electronic transitions.

Nanoparticles have a larger surface-to-volume ratio as compared to bulk phosphors.

This increases the interaction between optically active cations and the environment.

The particle size reduction leads to a critical increase in surface defects density, which plays a critical role in the brightness and storage capacity of the nanomaterials.

Bio-imaging was one of the first applications of persistent luminescent nanoparticles

(PLNPs). Unique delayed emission of PLNPs prevents living-tissue damage associated

with the simultaneous excitation with UV light required for most phosphors and

minimizes the interferences produced by the autofluorescence of tissues, hence leading

to an unprecedentedly high signal-over-noise ratio.

ZnGa₂O₄: Cr is an example of a persistent luminescent nanoparticle.

2.3. Mechanism

2.3.1 Crystal Field Splitting

The Cr^{+3} ion has a $3d^3$ electron configuration, and the outermost orbital is a 3d orbital.

The electron transition of Cr^{+3} ions is significantly affected by the crystal field. Since Cr^{+3} is in an octahedral symmetric environment 4F energy level splits- 4A_2 (ground state), 4T_2 , and 4T_1 . Excited state 4P splits into 4T_1 And 2G splits into 2E , 2T_1 , and 2T_2 .

When Cr^{+3} ions are in a strong crystal field environment, the 4T_2 energy level is higher than the 2E energy level, and the luminescence mainly originates from the spin-forbidden $^2E \rightarrow ^4A_2$ transition, [narrow-band NIR emission at around 700 nm.]

When Cr^{+3} ions are in a weak crystal field environment, the 4T_2 energy level is lower than the 2E energy level, and the luminescence originates from the spin-allowed $^4T_2 \rightarrow ^4A_2$ transition, (broad-band NIR emission of 650–1100 nm.) Therefore, we can regulate the emission of ZGC by adjusting the intensity of the ZnGa_2O_4 matrix crystal field.

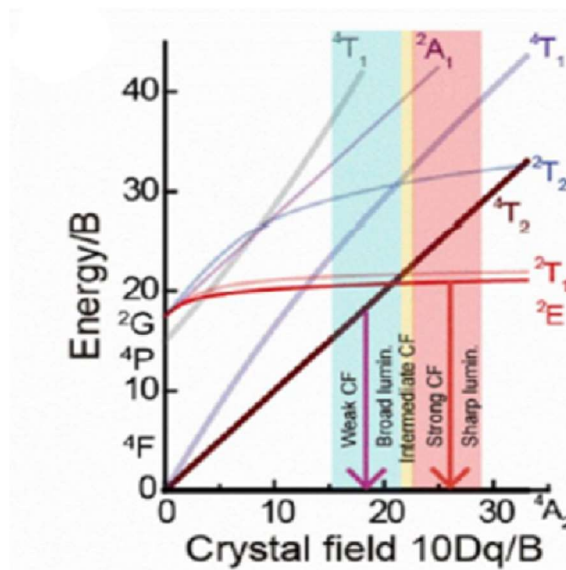
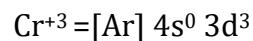
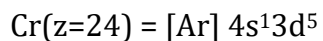


Figure 4: Energy level diagram of Cr^{3+} ion in the octahedral crystal field [2]

2.3.2 Persistent Luminescent Mechanism

According to the spin selection rule, the transition of Cr⁺³ ground-state ⁴A₂ to ⁴T₂, ⁴T₁ (t₂e), and ⁴T₁(te²) is allowed, corresponding to different excitation light wavelengths from UV to visible.

Process 1→Under UV excitation, the Cr⁺³ electrons transition from the ground-state energy level ⁴A₂ to the excited-state energy level ⁴T₁(te²), which is located near the bottom of the conduction band.

Process 2→Through thermal assistance, the electrons enter the conduction band and are then captured by nearby traps of different depths.

Process 3→ After the excitation stops, the electrons captured by the shallow trap enter the conduction band under the condition of external thermal stimulation and then return to the emission state ²E through non-radiative relaxation. Thereafter, they combine with the emitter Cr⁺³ to produce strong NIR emissions.

Process 4→ After a certain time, the electrons in the shallow trap are gradually exhausted, and the electrons in the deep trap return to the corresponding energy level through quantum tunnelling and combine with Cr⁺³, generating a long NIR emission.

Process 5→ Under low-energy light excitation, Cr⁺³ electrons transition from the ground-state energy level ⁴A₂ to the excited-state energy level ⁴T₁ (t²e) or ⁴T₂, which is far from the conduction band and electrons enter the nearby traps through quantum tunnelling.

Process 6→ After the excitation stops, the electrons in the trap return to the corresponding energy level through quantum tunnelling and combine with Cr⁺³, generating a NIR Emission.

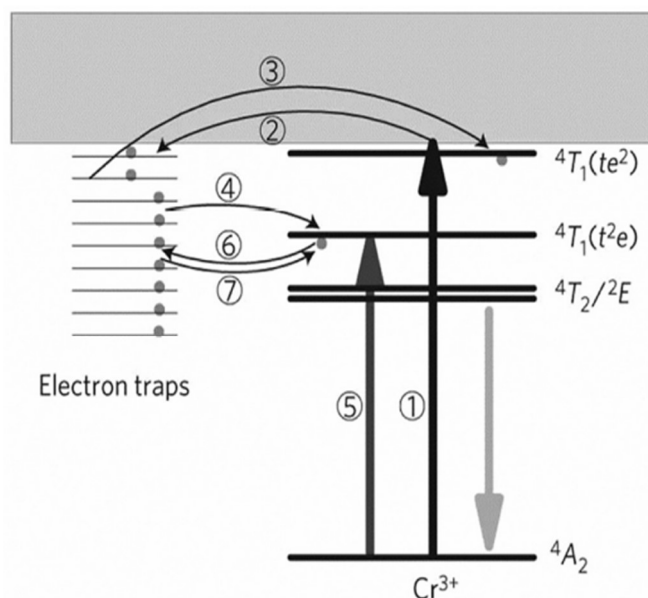


Figure 5: Schematic of the NIR Persistent Luminescence mechanism; 1–7 represent electron-transfer processes in ZGC [2]

2.3.3. Octahedral symmetry of Cr^{+3}

The elimination of the degeneracy of 3d orbitals separates d orbitals into two groups: t_{2g} (d_{xy} , d_{yz} , d_{zx}) and e_g (d_{z^2} and $d_{x^2-y^2}$). The electrons of Cr^{+3} in e_g orbitals are directed toward the negative lattice points in octahedral symmetry whereas the T_{2g} electrons of Cr^{+3} are directed between the point charges of the ligands. e_g has a greater energetic position than T_{2g} . 3 unpaired electrons in T_{2g} orbitals generate ${}^4A_{2g}$, 2E_g , ${}^2T_{1g}$. ${}^4A_{2g}$ is the ground state.

When one electron is excited to the e_g state, two quartet states (${}^4T_{1g}$ and ${}^4T_{2g}$) are formed. One quartet state ${}^4T_{1g}$ will be generated when two electrons are stimulated to the e_g state.

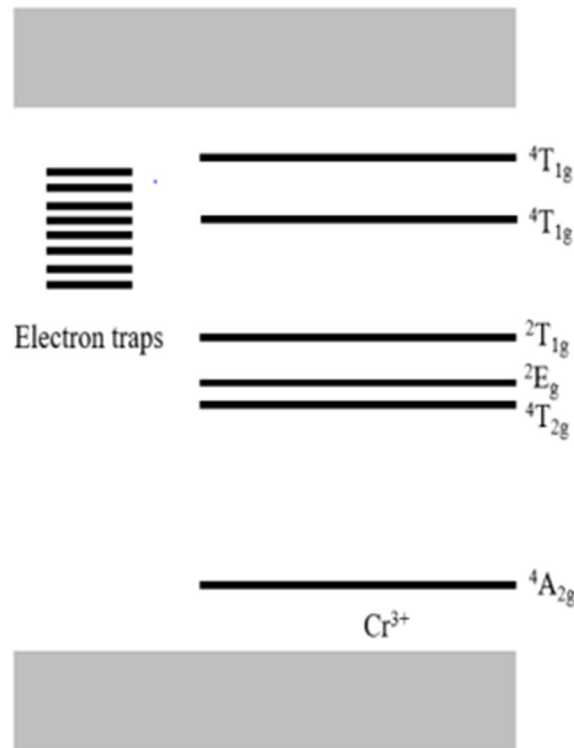


Figure 6: The energy diagram of Cr³⁺ in the octahedral symmetry. [3]

2.4. Factors Affecting Luminescence

2.4.1. Nature and Composition of Dopant

The metal-substituted zinc-gallates exhibited relevant emission colours depending on the dopant. Therefore, doping with different kinds of dopants give different emission wavelengths. Doping ZnGa₂O₄ with Cr³⁺ results in a red emission with a wavelength of around 700nm while ZnGa₂O₄: Mn²⁺ shows a green emission with a wavelength of around 500 nm.

Blending phosphors resulted in a whitish emission. Ji-Won Moon et al stated that a promising potential for white light is produced by biosynthesized mixtures of Cr-, Mn-, and Co- substituted zinc gallate representing RGB emissions.

Further Ji-Won Moon et al, showed that Mn-substituted zinc-gallates in which the Mn replaced either the Zn or Ga in nominal mole fraction precursor compositions produced

green light at 510 nm. Cr-substituted zinc gallates where the dopant replaced Ga produced red light at 705 nm. Eu-doped zinc gallate emitted the strongest emission at 615 nm and a secondary emission at 705 nm. The strongest RGB colours were emitted from the Cr 1%, Mn 4%, and Co 1% substituted zinc-gallates. Hence doping concentration greatly affects emission properties.

2.4.2 Effect of pH

Multiple noteworthy research papers concluded that the ideal pH is necessary for reaction mixtures to precipitate nanoparticles. Hydrothermal synthesis is a common method used to prepare spinel nanoparticles like ZnGa₂O₄. The process begins with the dissolving of metal precursor salts to produce hydroxy complexes. The hydroxy complexes react to form spinel nanoparticles at the microscopic level under the hydrothermal condition where the temperature is over 100°C at elevated pressures. A basic environment is essential for the production of Zn (OH)₃⁻ and Ga (OH)₄⁻ species. The concentration of OH plays a significant role in the reaction kinetics. NH₄OH is commonly used to adjust the pH for ZGO synthesis.

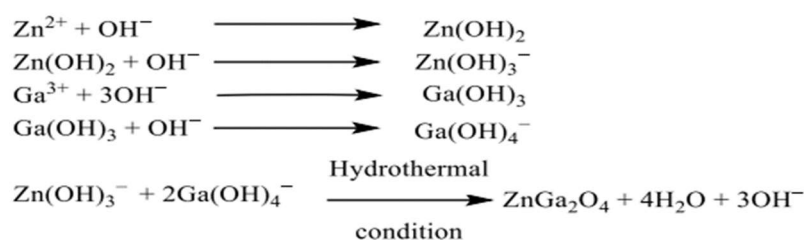


Figure 7: Chemical reaction to show formation of zinc gallate [3]

It was found that as the pH increased the particle size also increases well as its crystallinity. A low pH indicates a poor degree of crystallinity. It must be noted that the ideal pH for the preparation of zinc gallate is between a pH of 7 to 9. The product yield increases when the pH of the reaction mixture is very basic but pH above 9 results in

weaker photoluminescence.

pH value	7	9	11	9	9	9
Base addition rates	Medium	Medium	Medium	Slow	Medium	Fast
Crystal size (nm)	9.899	13.331	25.490	11.331	13.331	14.589

Table 1. The crystal sizes of Cr-ZGO prepared under different pH environments and different base addition rates ^[3]

2.4.3. Annealing temperature

Structural and optical properties of doped zinc gallate depend on the annealing temperature. Apart from resulting in larger particle sizes, higher annealing temperatures result in larger crystals with well-defined lattice constants and stronger photoluminescence. Undoped zinc gallate is expected to show weak photoluminescence before annealing but shows peaks of higher intensity post-annealing at temperatures between 700°C to 1000°C.

Annealing conditions determine the phase crystallinity of a material and have a visible effect on the persistent luminescent behaviour of the material. If dried at 150°C, ZnGa₂O₄: Cr⁺³ shows a faster luminescence intensity decay time due to defect resulting in a non-radiative loss. If the same material is annealed at 1000°C, it would show a longer luminescence intensity decay time because of the absence of defects that cause non-radiative losses. This can also be seen when Mn⁺² is the dopant wherein annealing led to the activation of the radiative route.

2.4.4 Effect of excitation wavelength

The exciting wavelength is crucial and dependent on the applications of the sample. For $\text{ZnGa}_2\text{O}_4: \text{Cr}^{+3}$, we used UV excitation of wavelengths 254nm and 400 nm as well as 532 nm to obtain an NIR emission. Literature review shows that excitation with X-rays proves to be efficient where in vivo excitation is required. Other excitations, i.e., red/white, UV and NIR, can be used for applications that require ex-vivo applications.

CHAPTER 3: SYNTHESIS

3. Synthesis

3.1. Methods of Synthesis

Synthesis of nanomaterials follows two major approaches; the top-to-bottom approach and the bottom-to-top approach. The sol-gel method and the hydrothermal method are examples of the bottom-to-top approach. The synthesis method chosen plays a significant role in the properties and physical dimensions of the sample. The bottom-up approach is the method in which the components of atomic or molecular dimensions are assembled to form nanoparticles. The bottom-up method is much more used for the preparation of nanoparticles because it allows controlling their size.

3.1.1. Sol-Gel Method.

The Sol-Gel method is a wet chemical technique that is commonly used to prepare nanomaterials. It results in products with good purity, and homogeneity and yields stoichiometric powders at relatively low annealing temperatures. It is to be noted that products obtained for sol-gel synthesis are found to be highly agglomerated and morphologically irregular. This is because of uncontrol over the nanoparticle growth stage.

We initially used the Sol-Gel method to synthesize undoped Zinc Gallate. [5]

ZnGa₂O₄ nanoparticles were synthesized at room temperature using zinc acetate and gallium nitrate as starting materials. Initially, 1.0g of Zn (Ac)₂·2H₂O was dissolved in 100 ml of boiling ethanol (76-78° C) at atmospheric pressure under stirring. After 60 minutes, 150 ml of distilled water was added. The solution remained under stirring for 30 minutes. Then, 1.0g of gallium nitrate was added, yielding a transparent solution.

The molar ratio Ga/Zn was almost equal to 1. This gives a transparent solution. 0.3g of

LiOH was then added and the nanoparticles were formed and then precipitated. Centrifugation and washing were repeated several times. The precipitate was then dried for 24h at 40°C under a vacuum. The obtained dried product was then annealed at 700°C.

The sol-gel method is important in the production of nanoparticles because of the ease of synthesis and short reaction times. We must note that for small particle sizes, the sol-gel method does not work well since the technique usually leads to large particle sizes. Adjustment of pH is also a factor that affects the properties of the nanomaterials. Such adjustment is difficult to do in a sol-gel method.

3.1.2. Hydrothermal Method

The Hydrothermal method is most commonly used in the preparation of nanomaterials. It refers to the heterogeneous reaction of inorganic materials to form crystals by solubility changes of substances in the sealed aqueous solution above ambient room temperature and pressure. This method is very suitable for synthesizing nano-size particles which are fundamental for biological applications. It produces a powder material with high chemical purity. The crystallization step tends to reject impurities that occur in the growth environment. This means we are expected to remove the impurities such as ions coming from metal salts or PH adjusting from the system along with the crystallization solution.

We prepared all our samples using the hydrothermal process since it offers high yield, easy size control, easy pH adjustment, uniform morphology, and excellent dispersion of product. The main parameters of hydrothermal synthesis, which define both the

process kinetics and the properties of the resulting products are the initial pH of the solution, the duration, the temperature of the synthesis, and the pressure in the system.

3.2 Sample Preparation

We prepared the following samples using the hydrothermal process. Advantages of this method include low-temperature requirement as compared to solid state reaction, cheap cost, and no requirement for chemical catalyst.

1. ZnGa_2O_4
2. $\text{ZnGa}_{1.993}\text{Cr}_{0.007}\text{O}_4$
3. $\text{ZnGa}_{1.995}\text{Ni}_{0.005}\text{O}_4$
4. $\text{ZnGa}_{1.995}\text{Co}_{0.005}\text{O}_4$
5. $\text{ZnGa}_{1.77}\text{Mn}_{0.224}\text{O}_4$

3.2.1 List of chemicals

Name	Chemical Formula	Purity	Molecular Weight	Supplier
Zinc Nitrate Hexahydrate	$\text{Zn}(\text{NO}_3)_2 \cdot 6\text{H}_2\text{O}$	99.99%	297.52	Sigma-Aldrich
Gallium Nitrate Hydrate	$\text{Ga}(\text{NO}_3)_3 \cdot x\text{H}_2\text{O}$	99.99%	255.73	Sigma-Aldrich
Chromium Nitrate Nonahydrate	$\text{Cr}(\text{NO}_3)_3 \cdot 9\text{H}_2\text{O}$	99.99%	400.15	Sigma-Aldrich
Cobalt Nitrate Hexahydrate	$\text{Co}(\text{NO}_3)_2 \cdot 6\text{H}_2\text{O}$	99.99%	291.04	Sigma-Aldrich
Nickel Nitrate Hexahydrate	$\text{Ni}(\text{NO}_3)_2 \cdot 6\text{H}_2\text{O}$	99.99%	290.8	Sigma-Aldrich

Table 2. List of chemicals

3.2.2. Calculation for respective sample preparations

1. ZnGa_2O_4

Molecule	Stoichiometric Ratio	Required Weight (g)
$\text{Zn}(\text{NO}_3)_2 \cdot 6\text{H}_2\text{O}$	1	0.3719
$\text{Ga}(\text{NO}_3)_3 \cdot x\text{H}_2\text{O}$	2	0.6393

Table 3. Calculation for preparation of Zinc Gallate

2. $\text{ZnGa}_{1.993}\text{Cr}_{0.007}\text{O}_4$

Molecule	Stoichiometric Ratio	Required Weight (g)
$\text{Zn}(\text{NO}_3)_2 \cdot 6\text{H}_2\text{O}$	1	0.3719
$\text{Ga}(\text{NO}_3)_3 \cdot x\text{H}_2\text{O}$	1.993	0.6393
$\text{Cr}(\text{NO}_3)_3 \cdot 9\text{H}_2\text{O}$	0.007	0.04001

Table 4. Calculation for preparation of Cr doped Zinc Gallate

3. $\text{ZnGa}_{1.995}\text{Ni}_{0.005}\text{O}_4$

Molecule	Stoichiometric Ratio	Required Weight (g)
$\text{Zn}(\text{NO}_3)_2 \cdot 6\text{H}_2\text{O}$	1	0.3719
$\text{Ga}(\text{NO}_3)_3 \cdot x\text{H}_2\text{O}$	1.995	0.6393

Ni (NO ₃) ₂ .6H ₂ O	0.005	0.029080
---	-------	----------

Table 5. Calculation for preparation of Ni doped Zinc Gallate

4. ZnGa_{1.995}Co_{0.005}O₄

Molecule	Stoichiometric Ratio	Required Weight (g)
Zn (NO ₃) ₂ .6H ₂ O	1	0.3719
Ga (NO ₃) ₃ . xH ₂ O	1.995	0.6393
Co (NO ₃) ₂ .6H ₂ O	0.005	0.029103

Table 6. Calculation for preparation of Co doped Zinc Gallate

5. ZnGa_{1.77}Mn_{0.224}O₄

Molecule	Stoichiometric Ratio	Required Weight (g)
Zn (NO ₃) ₂ .6H ₂ O	1	0.3719
Ga (NO ₃) ₃ . xH ₂ O	1.77	0.6393
Mn (NO ₃) ₂ .2H ₂ O	0.224	0.017895

Table 7. Calculation for preparation of Mn doped Zinc Gallate

3.2.3. Procedure

- 0.0025 mol of $\text{Ga}(\text{NO}_3)_3 \cdot x\text{H}_2\text{O}$ and 0.00125 mol of $\text{Zn}(\text{NO}_3)_2 \cdot 6\text{H}_2\text{O}$ was dissolved in 5 ml of distilled water in 2 separate beakers. When the zinc nitrate and gallium nitrate were dissolved, the zinc nitrate solution was dissolved into the gallium nitrate solution by stirring vigorously.
- Preparation of the stock solution is only needed when doping zinc gallate and is not used in the undoped case. We explain the preparation of the stock solution for the case of chromium, the same can then be utilized with appropriate changes in the nitrate used depending on the desired dopant.
- A stock solution of chromium nitrate was made by mixing 0.0001 mol (0.040015g) of chromium nitrate into 10 ml of distilled water. 500 μL of this stock solution was pipetted out into the gallium-zinc solution.
- The mixture was then stirred for 30 minutes using a magnetic stirrer. The pH of the solution was adjusted to pH 8. This was done by adding ammonium hydroxide drop by drop. The solution is stirred during the pH adjustment. The resulting pH 8 mixture was transferred to a Teflon autoclave and heated in the oven for 20-22 hours at 160°C.
- When the solution is cooled to room temperature, the precipitate was collected by centrifuge.
- 5mL of 0.1M HCl is added to the centrifuge tube, and the centrifuge tube is shaken to wash the precipitate. The precipitate is separated by centrifuge. Acid washing is important to remove any possible ZnO impurities that can be present.
- 10mL of 2-propanol was then added to further wash the sample. After addition, the sample was centrifuged and the supernatant was discarded.

- The precipitate was collected, air-dried, and characterized.
- Each of the prepared samples were annealed at 800°C. The temperature was raised at a rate 5°C per minute and kept at 800°C for 4 hours and then cooled to room temperature at the same rate.

Chapter- 4:

Characterization & Results

4. Characterization Methods

The samples were characterised and studied using the following characterisation techniques.

- X-ray diffraction
- Scanning Electron Microscopy
- UV Visible Spectroscopy
- Photoluminescent Spectroscopy

4.1. X-ray Diffraction

X-ray diffraction is a non-destructive technique that provides detailed information about the crystallographic structure, chemical composition, and physical properties of materials. This method of characterisation was carried out to confirm the formation of zinc gallate based samples. It was also used to find the lattice parameter and the average crystallite size.

The method takes advantage of the fact that X-ray wavelengths are similar to the interatomic spacing of crystalline solids and hence the angle of diffraction will be affected by the spacing of the atoms in the molecules. This would not be possible with larger wavelengths as they would be unaltered by the spacing.

Bragg condition states that, X-rays scattered from different crystal planes produce diffraction when the path difference between the waves is equal to the integer multiple of the X-ray wavelength formulated as $2d_{hkl}\sin\theta = n\lambda$, where n is an integer, λ is the incident wavelength, d_{hkl} is the lattice spacing, n is an integer which represents order of diffraction, and θ is the angle of diffraction.

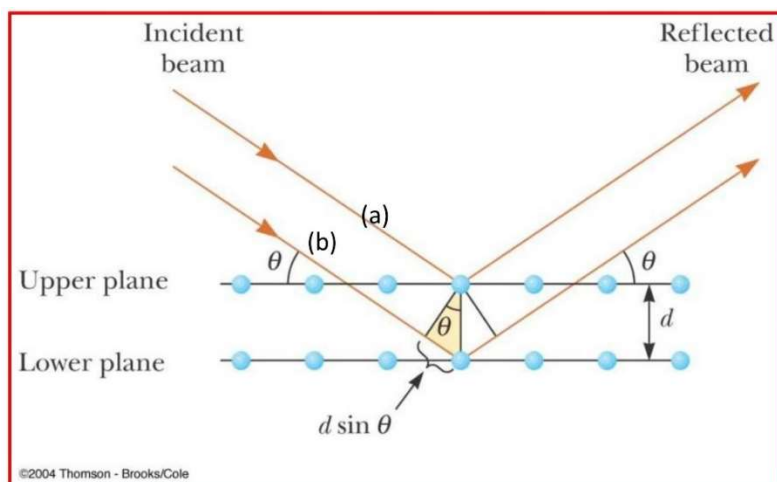


Figure 8: Diffraction of Xray beam through a crystal [16]

Hence a diffraction pattern is obtained when the path difference between the incident and scattered wave matches and is unique for a given crystal. Different diffraction patterns are obtained for different crystals because of the difference in d_{hkl} . By analysing a plot of diffracted intensity v/s 2θ we can obtain necessary information.

X-ray Diffraction measurements were performed using Cu- K_{α} radiation source of wavelength $\lambda=1.54\text{\AA}$. Each of the samples were ground to a fine powder before performing the measurement. The following are our results:

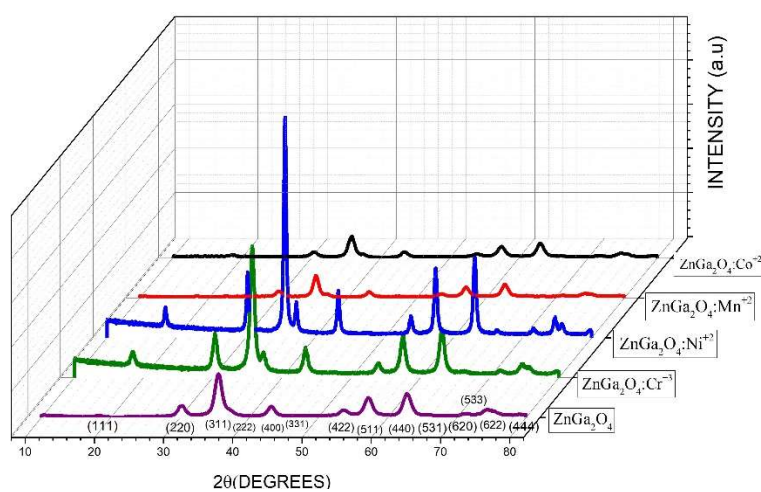


Figure 9: XRD pattern of zinc gallate and Cr, Ni, Co, and Mn doped Zinc Gallates before annealing.

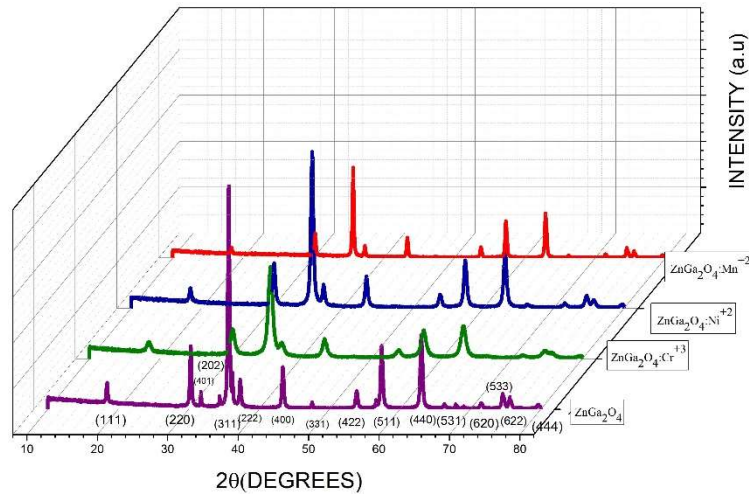


Figure 10: XRD pattern of zinc gallate and Cr, Ni, Co, and Mn doped Zinc Gallates after annealing.

The XRD peaks match with literature and served as a confirmation on formation of product. On comparing diffraction peaks of the annealed samples with that which were not annealed, we see the presence of two additional peaks (401) and (202). This agrees with literature and is because of the phase separation of zinc gallate. The intensity of the diffraction peak (311) increased on annealing as is evident from the above graphs.

Further, we analysed the data and found the lattice parameter of each prepared sample as well as the crystallite size. The crystallite size was calculated using the Debye Scherrer equation.

$$D = \frac{K\lambda}{\beta \cos \theta}$$

where, D represents the nanoparticle crystallite size, λ is the radiation source wavelength, θ is the Bragg angle in degrees, β is the line broadening at full width half maximum (FWHM), and K is Scherrer constant. K can take values between 0.68 to 2.08 but for our case $K=0.94$ since we deal with a spherical crystallite with cubic symmetry.

Below mentioned are the calculated lattice parameter (a) and crystallite size (D) and interplanar distance (d).

Sample	Before Annealing			After Annealing		
	D(Å)	d(Å)	a (nm)	D(Å)	d(Å)	a(nm)
ZnGa₂O₄	10.62	2.98	8.33	20.13	2.12	7.05
ZnGa₂O₄: Cr⁺³	11.09	2.49	8.27	22.90	2.10	6.97
ZnGa₂O₄: Ni⁺²	10.49	2.52	8.34	24.61	2.09	6.94
ZnGa₂O₄: Co⁺²	13.37	2.60	8.65	-	-	-
ZnGa₂O₄: Mn⁺²	15.57	2.38	7.90	24.04	2.18	7.24

Table 8: Crystallite size, interplanar distance and lattice parameter, before and after annealing.

From the tabular data above, we conclude that the crystallite size increases due to coalescence during thermal treatment. Annealing provides sufficient driving force to improve mobility of the atoms and improve the crystallinity.

4.2. Scanning Electron Microscopy

Scanning Electron Microscopy is a very useful investigative tool that uses a focused beam of electrons to produce complex, high magnification images of a sample's surface topography. Using SEM, we can find the particle size of each sample. SEM creates an image by detecting reflected or knocked-off electrons. On analysing each sample, the following was observed. The particle sizes are seen to be below 100nm.

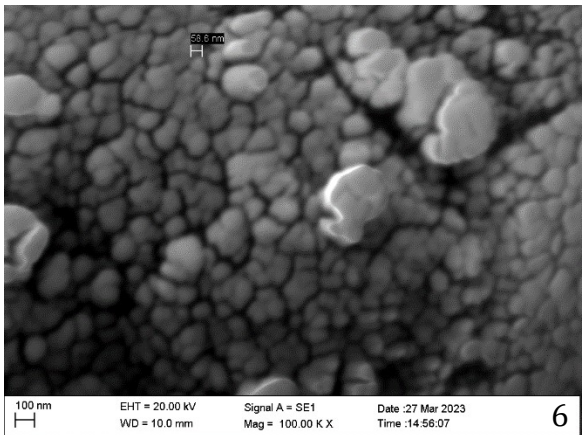
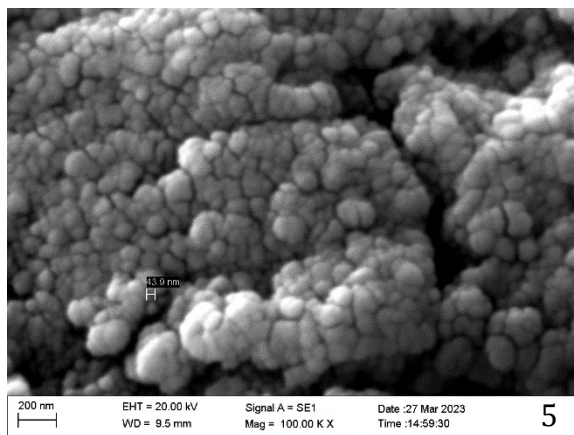
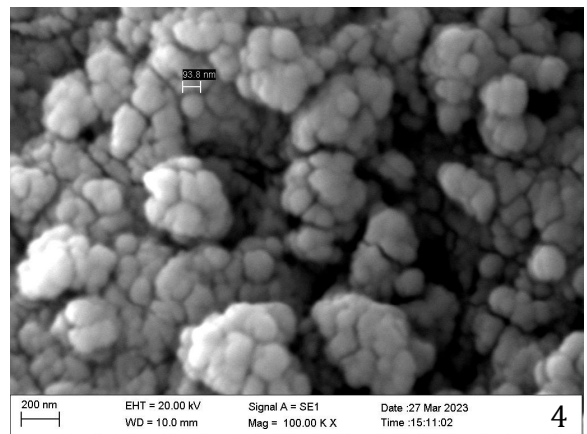
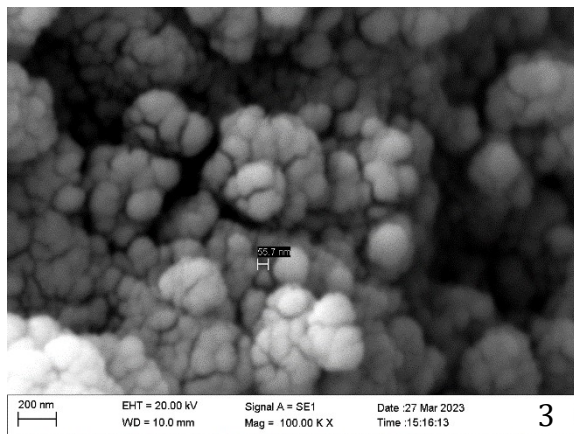
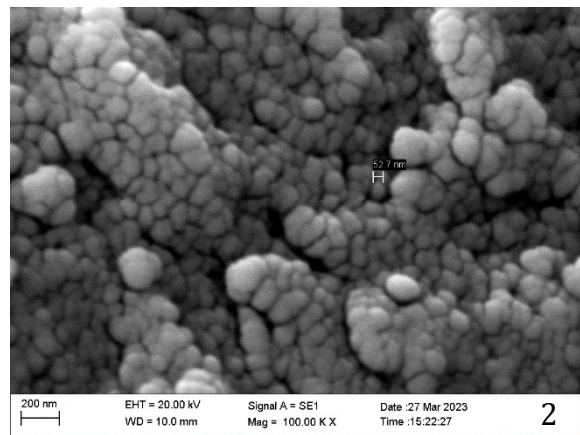
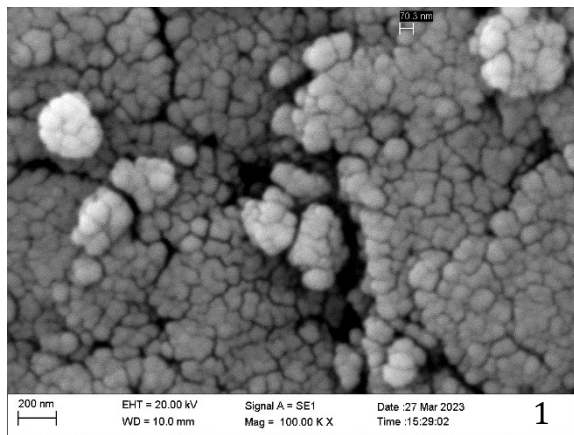


Figure 11: SEM images of 1) Ni annealed, 2) Annealed Undoped, 3) Annealed Cr doped, 4) Cr doped, 5) Undoped, 6) Ni doped Zinc gallate.

The average size of the particles was also obtained from histograms.

4.3 UV Visible Spectroscopy

UV Visible Spectroscopy is an analytical technique that measures the amount of discrete wavelengths of UV or visible light that are absorbed by or transmitted through a sample in comparison to a reference or blank sample.

It is based on the principle that when light falls on a substance it absorbs part of the light and reflects part of it. Hence the amount of radiation absorbed is the difference between the incident and transmitted radiation. According to Beer Lambert's Law, the absorbance of a solution is directly proportional to the concentration of the absorbing species and the path length. The measurement is carried out by dissolving the sample in distilled water and pouring it into a cuvette which is then placed in the sample compartment. Standard cuvettes are made of glass, quartz or plastic and allow easy transmittance of ultraviolet radiation. Using the optical absorption spectra so obtained, we can calculate the band gap of the sample by the Tauc's formula,

$$(\alpha h\nu)^\gamma = A(h\nu - E_g)$$

Where α is the absorption coefficient, h is planks constant, ν is the frequency, A is a proportionality constant, and $\gamma=0.5$ as we have an indirect band gap. The absorption spectra and respective tauc plots were used to find the band gap of the samples.

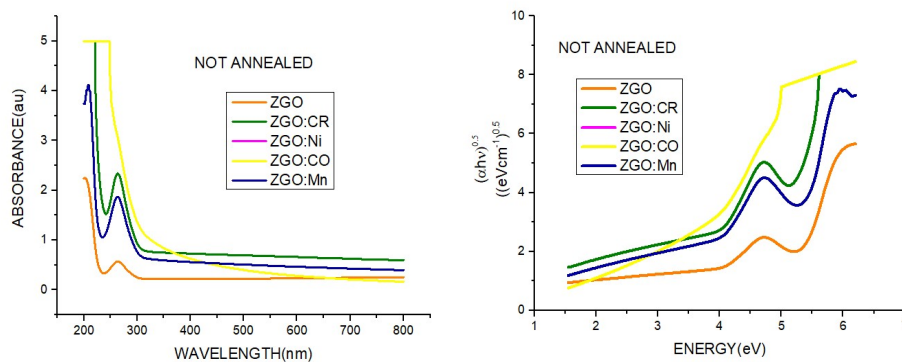


Figure 12: Absorption spectra and tauc plot for samples before annealing.

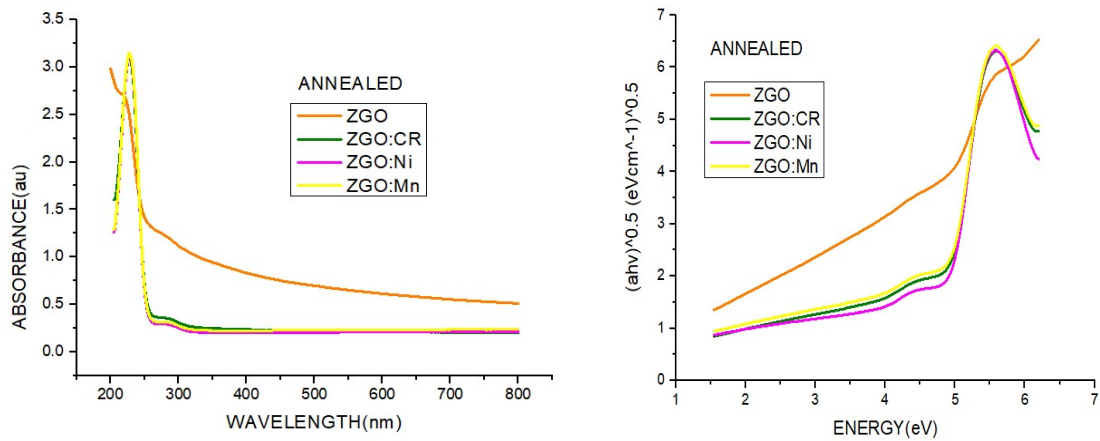


Figure 13: Absorption spectra and tauc plot for samples after annealing.

Sample	Band Gap (Before Annealing) (eV)	Band Gap (After Annealing) (eV)
ZnGa ₂ O ₄	4.87	4.02
ZnGa ₂ O ₄ : Cr ⁺³	4.75	4.67
ZnGa ₂ O ₄ : Ni ⁺²	4.85	4.79
ZnGa ₂ O ₄ : Co ⁺²	4.35	-
ZnGa ₂ O ₄ : Mn ⁺²	4.86	4.78

Table 9: The change in band gap before and after annealing.

The choice of dopant is made in such a way that the resulting sample after doping had a band gap within the band gap of the parent sample. Hence the band gaps of the doped samples are smaller than that of the parent sample.

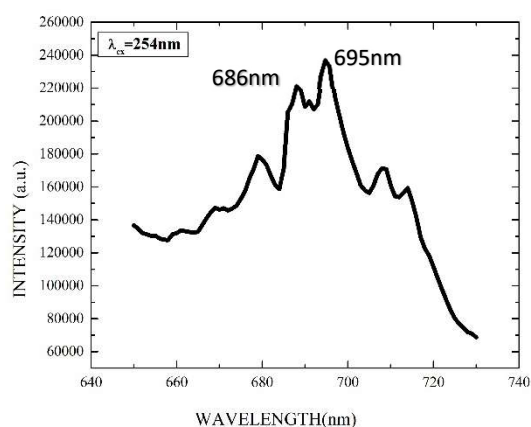
We also observe a decrease in the band gap on annealing. Multiple reports suggest that the decrease in the band gap is because of increase in the crystallite size as well as decreasing defect concentration on annealing. Others suggest that the decrease is a result of decrease in intermediary energy levels.

The introduced dopant energy levels tend to mix with the original energy bands of the semiconductor. This mixing leads to broadening of the energy bands and consequently, a reduction in the effective band gap. Hence more electrons will move to the conduction band easily thereby improving the persistent luminescence.

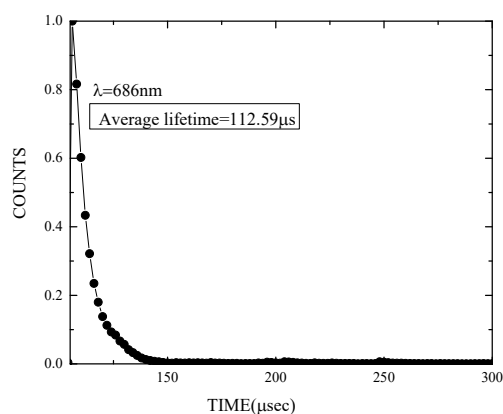
4.3. Photoluminescent Spectroscopy

Photoluminescent Spectroscopy is a type of light emission spectroscopy. The emission spectrum is obtained by exciting electrons at a fixed wavelength and observing emissions at different wavelengths. When light of a particular wavelength is incident onto a sample, electrons absorb energy and transition to excited states. They release energy in the form of light as they de-excite.

Photoluminescent spectroscopy was conducted for $\text{ZnGa}_2\text{O}_4: \text{Cr}^{+3}$ at three different excitation wavelengths i.e., 254nm, 400nm and 532nm. Excitation wavelengths were chosen in such a way that they correspond to d-d absorption band of Cr^{+3} ions.



(a)



(b)

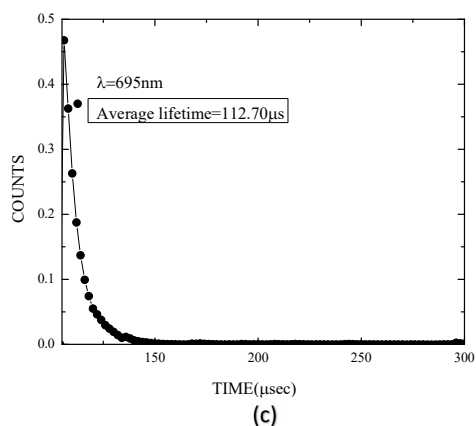


Figure 14: a) Emission Spectrum of ZGC at $\lambda_{ex}=254\text{nm}$, Phosphorescence decay at b)686nm shows as average lifetime of $112.59\mu\text{s}$ and c)695nm shows an average lifetime of $112.70\mu\text{s}$.

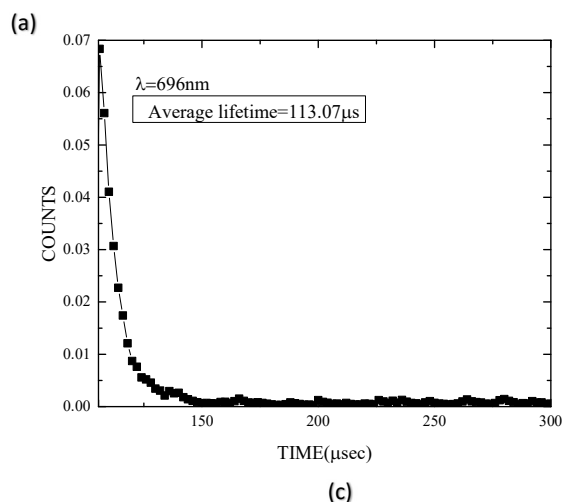
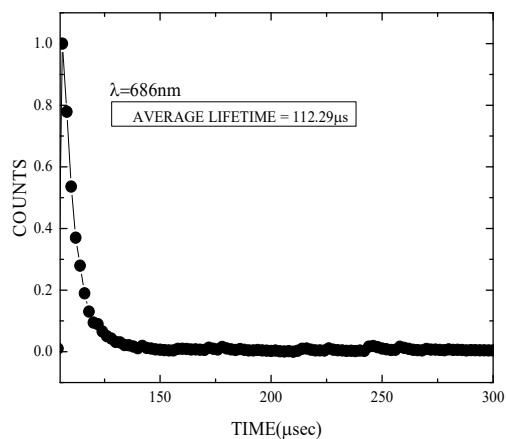
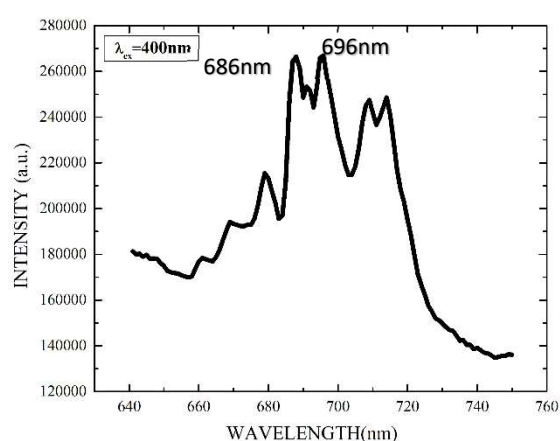


Figure 15: a) Emission Spectrum of ZGC at $\lambda_{ex}=400\text{nm}$, Phosphorescence decay at b)686nm shows as average lifetime of $112.29\mu\text{s}$ and c)696nm shows an average lifetime of $113.07\mu\text{s}$.

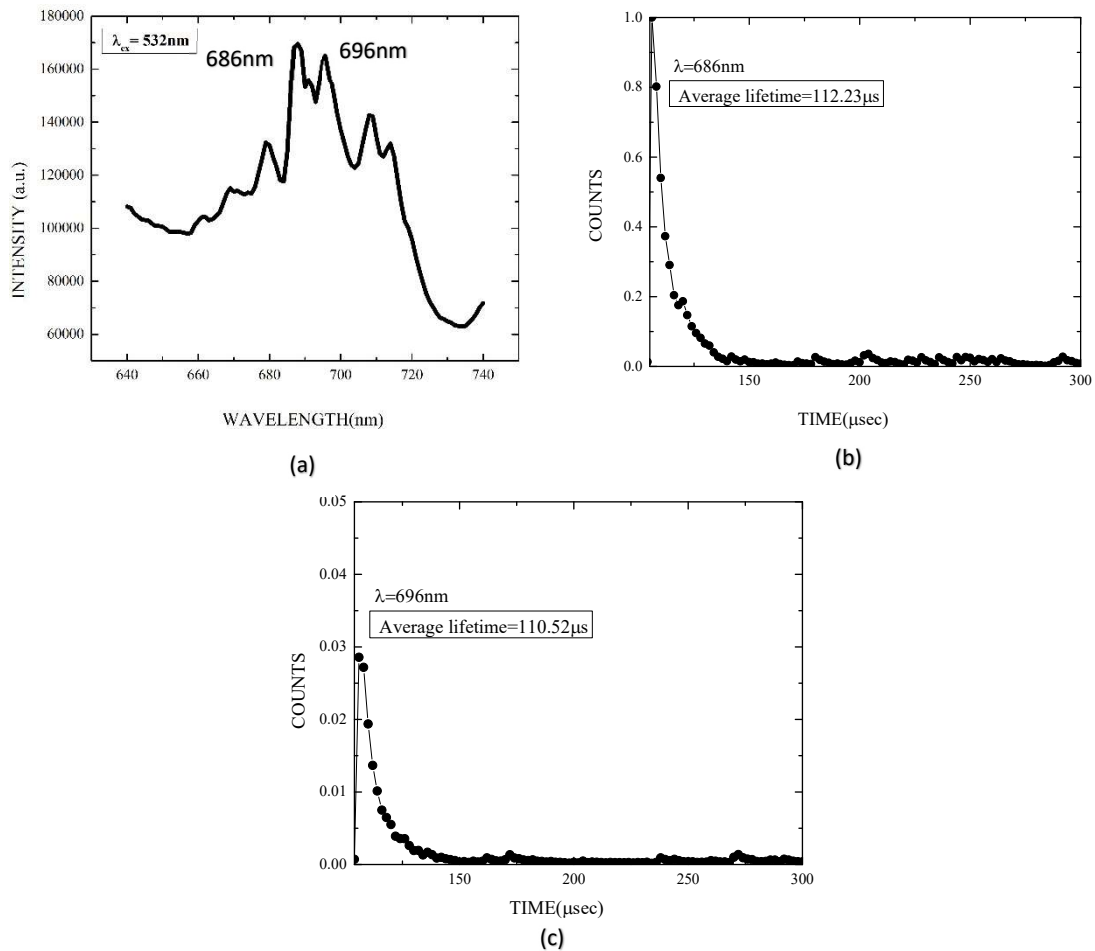


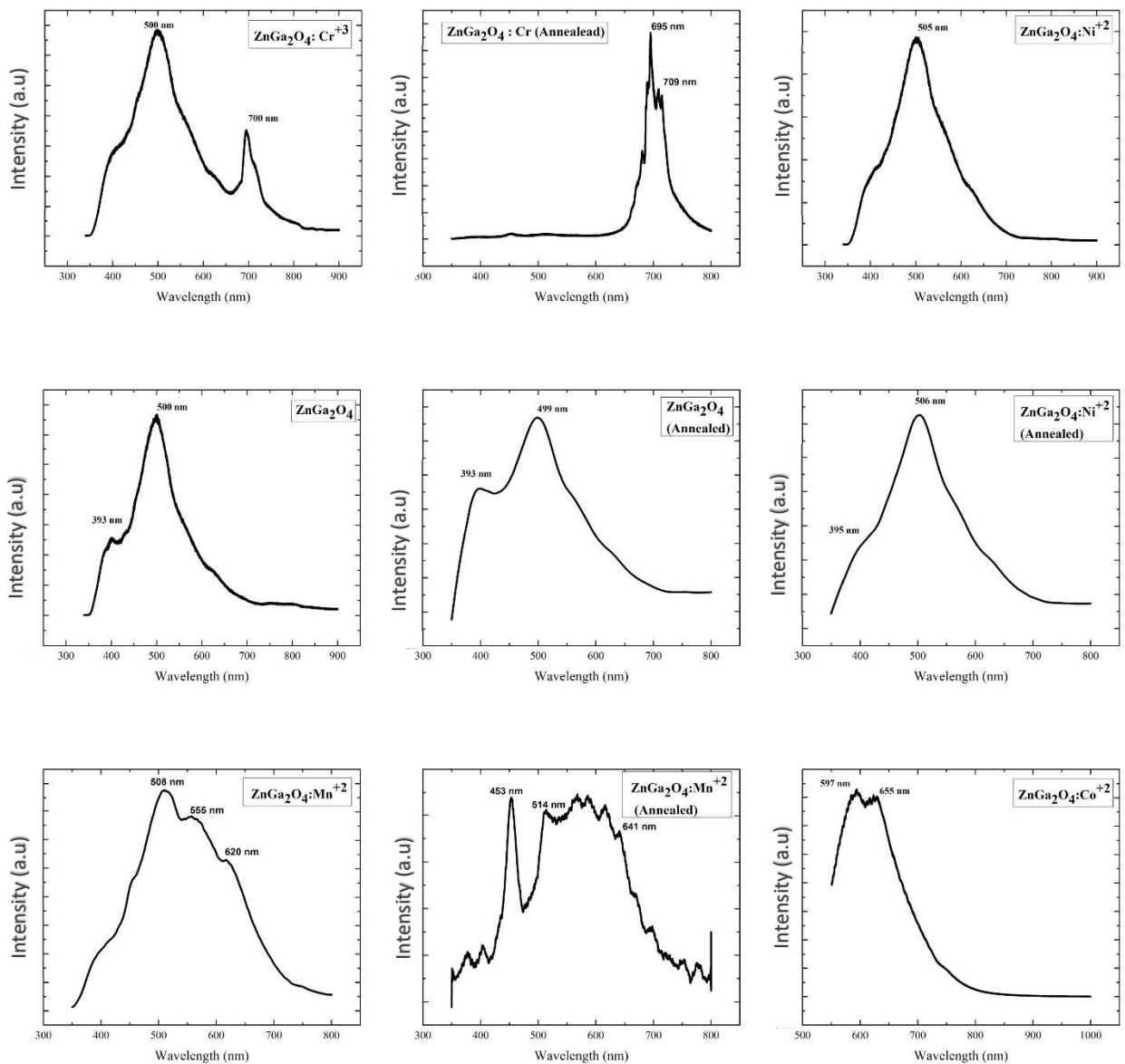
Figure 16: a) Emission Spectrum of ZGC at $\lambda_{ex}=532\text{nm}$, Phosphorescence decay at b)686nm shows as average lifetime of 112.23 μs and c)696nm shows an average lifetime of 110.52 μs .

For 254nm prominent peaks were obtained at 695nm and 686nm. For 400nm and 532nm prominent peaks were obtained at 686nm and 696nm. The first peak in each case is due to the d-d transition from ${}^2E - {}^4A_2$ level. This is also called the R phonon line. The R phonon line shows phonon side bands called stokes lines above 700nm and anti-stokes lines below 686nm. The second peak represents the N_2 band which is due to the Cr^{+3} ions which are distorted by the antisite defect.

Phosphorescence decay studies were conducted by using excitation wavelength comparable to the above-mentioned peaks and obtained the respective decay times

which are seen to exist in the range of 110 μ s to 113 μ s. This represents the average lifetime of the sample in the respective transitions.

Photoluminescent measurements were also performed using laser excitation of 234nm and 532 nm. Prominent peaks, one as a result of zinc gallate and the other when doped appear in each case in the range of 450nm to 700nm.



Chapter-5: Conclusion

5.1 APPLICATIONS

Zinc gallate doped with chromium (ZGC) can produce near infrared persistent luminescence which avoids tissues autofluorescence as well as has a high tissue penetration depth and hence finds great use in bio-imaging. ZGC has been reported to have remarkable in vivo re-excitability. Biological tests have been conducted on mice wherein such nanoparticles have been injected via the tail vein and with ability of in-vivo excitation by a white LED.

The excitation wavelength is crucial in the case of in-vivo excitation. UV-excited ZGC NP's can be used for applications involving ex-vivo excitation as in-vivo excitation post decay is difficult and may result in a decrease in image sensitivity. White/red light can be excited in-vivo but they have a short wavelength and are not suitable for excitation in deep tissue. Therefore, for effective in-vivo excitation, we need a light source which shows sufficient tissue penetration and can re-excite the ZGC even in deeper tissues. It is for these reasons that X-rays are used. Their use is not limited by depth of tissue. ZGC excited in-vivo with X-rays can be used in highly sensitive tumour imaging.

5.2 CONCLUSION

Zinc gallate nanoparticles were successfully synthesised using the hydrothermal method. The parent compound was successfully doped, using the same synthesis method, with chromium, cobalt, nickel, and manganese. Each of the samples were confirmed by X-ray diffraction. The average crystallite size is found to be 12.28 nm and was found to increase on annealing. The band gap was calculated using absorption spectra obtained from UV Visible spectroscopy. The average band gap is 4.7 eV and is seen to decrease on annealing. The band gap also differs, although to a small extent, between samples doped with different dopants. SEM confirmed the nanoparticle size

which increased on annealing. Photoluminescent spectroscopy gave peaks at 686nm and 696nm for ZGC. A phosphorescence decay time was obtained at the wavelengths for excitation wavelengths of 254nm, 400nm, 532 nm. Peaks for other samples were found to in the range of 450nm to 650nm.

Further studies can be carried out with respect to the samples prepared. One can vary the annealing temperature and observe the respective changes or vary the pH to show a change in yield and photoluminescent properties. Different other transition metals like Al^{+3} can be used as dopants. Persistent luminescent decay can be measured for each of the prepared samples to verify its occurrence in such compounds.

BIBLIOGRAPHY

1. Bessière, A., Sharma, S. K., Basavaraju, N., Priolkar, K. R., Binet, L., Viana, B., ... Gourier, D. (2014). *Storage of Visible Light for Long-Lasting Phosphorescence in Chromium-Doped Zinc Gallate*. *Chemistry of Materials*, 26(3), 1365–1373. doi:10.1021/cm403050q
2. Sun, X., Song, L., Liu, N., Shi, J., & Zhang, Y. (2021). *Chromium-Doped Zinc Gallate Near-Infrared Persistent Luminescence Nanoparticles in Autofluorescence-Free Biosensing and Bioimaging: A Review*. *ACS Applied Nano Materials*, 4(7), 6497–6514. doi:10.1021/acsanm.1c01115
3. Li, Xincheng, "Investigating the Influence of Synthetic Environments on the Electronic Structure and Luminescence of Cr-doped Zinc Gallate" (2022). *Electronic Thesis and Dissertation Repository*. 8663. <https://ir.lib.uwo.ca/etd/8663>
4. Li, L., Wang, Y., Huang, H., Li, H., & Zhao, H. (2016). *Long-lasting luminescence in ZnGa₂O₄: Cr³⁺ through persistent energy transfer*. *Modern Physics Letters B*, 30(04), 1650019. doi:10.1142/s0217984916500196
5. *ACS Appl. Nano Mater.* 2022, 5, 7, 8950–8961
6. Tan, H., Wang, T., Shao, Y., Yu, C., & Hu, L. (2019). *Crucial Breakthrough of Functional Persistent Luminescence Materials for Biomedical and Information Technological Applications*. *Frontiers in Chemistry*, 7. doi:10.3389/fchem.2019.00387
7. Li, Z., Zhang, Y., Wu, X., Huang, L., Li, D., Fan, W., & Han, G. (2015). *Direct Aqueous-Phase Synthesis of Sub-10 nm "Luminous Pearls" with Enhanced in Vivo Renewable Near-Infrared Persistent Luminescence*. *Journal of the American Chemical Society*, 137(16), 5304–5307. doi:10.1021/jacs.5b00872

8. Wu, S., Li, Y., Ding, W., Xu, L., Ma, Y., & Zhang, L. (2020). *Recent Advances of Persistent Luminescence Nanoparticles in Bioapplications*. *Nano-Micro Letters*, 12(1). doi:10.1007/s40820-020-0404-8
9. Loeffler, L., & Lange, F. F. (2004). *Hydrothermal Synthesis of Undoped and Mn-Doped ZnGa₂O₄ Powders and Thin Films*. *Journal of Materials Research*, 19(03), 902–912. doi:10.1557/jmr.2004.19.3.902
10. Silva, M. N. da, Miranda de Carvalho, J., Fantini, M. C. de A., Chiavacci, L. A., & Bourgaux, C. (2019). *Nanosized ZnGa₂O₄:Cr³⁺ Spinels as Highly Luminescent Materials for Bioimaging*. *ACS Applied Nano Materials*. doi:10.1021/acsanm.9b01417
11. Srivastava, B. B., Kuang, A., & Mao, Y. (2015). *Persistent luminescent sub-10 nm Cr doped ZnGa₂O₄ nanoparticles by a biphasic synthesis route*. *Chemical Communications*, 51(34), 7372–7375. doi:10.1039/c5cc00377f
12. Mondal, A., Das, S., & Manam, J. (2019). *Investigation on spectroscopic properties and temperature dependent photoluminescence of NIR emitting Cr³⁺ doped zinc gallate long persistent nanophosphor*. *Physica B: Condensed Matter*. doi:10.1016/j.physb.2019.05.030
13. Batista, M.S.; Rodrigues, J.; Relvas, M.S.; Zanoni, J.; Girão, A.V.; Pimentel, A.; Costa, F.M.; Pereira, S.O.; Monteiro, T. Optical Studies in Red/NIR Persistent Luminescent Cr-Doped Zinc Gallogermanate (ZGGO:Cr). *Appl. Sci.* 2022, 12, 2104. <https://doi.org/10.3390/app12042104>
14. Dutta, D. P., Ghildiyal, R., & Tyagi, A. K. (2009). Luminescent Properties of Doped Zinc Aluminate and Zinc Gallate White Light Emitting Nanophosphors Prepared via Sonochemical Method. *The Journal of Physical Chemistry C*, 113(39), 16954–16961. doi:10.1021/jp905631g

15. Chen, M.-I., Singh, A. K., Chiang, J.-L., Horng, R.-H., & Wu, D.-S. (2020). *Zinc Gallium Oxide—A Review from Synthesis to Applications*. *Nanomaterials*, 10(11), 2208. doi:10.3390/nano10112208
16. Thomson-Brooks/Cole, College Physics, Pacific Grove, CA, ©2003
17. Victor Castaing, Encarnación Arroyo, Ana I. Becerro, Manuel Ocaña, Gabriel Lozano, Hernán Míguez; Persistent luminescent nanoparticles: Challenges and opportunities for a shimmering future. *Journal of Applied Physics* 28 August 2021; 130 (8): 080902. <https://doi.org/10.1063/5.0053283>
18. Moon, J.-W., Kim, J. S., Park, J. H., Ivanov, I. N., & Phelps, T. J. (2019). *Synthesis of zinc-gallate phosphor by biomineralization and their emission properties*. *Acta Biomaterialia*. doi:10.1016/j.actbio.2019.07.052
19. Tuerdi, A., & Abdukayum, A. (2019). Dual-functional persistent luminescent nanoparticles with enhanced persistent luminescence and photocatalytic activity. *RSC Advances*, 9(31), 17653–17657. doi:10.1039/c9ra02235j
20. MODAN, E.M. and PLĂIAȘU, A.G. 2020. Advantages and Disadvantages of Chemical Methods in the Elaboration of Nanomaterials. *The Annals of "Dunarea de Jos" University of Galati. Fascicle IX, Metallurgy and Materials Science*. 43, 1 (Mar. 2020), 53-60. DOI:<https://doi.org/https://doi.org/10.35219/mms.2020.1.08>.
21. Chen, M.-I., Singh, A. K., Chiang, J.-L., Horng, R.-H., & Wu, D.-S. (2020). *Zinc Gallium Oxide—A Review from Synthesis to Applications*. *Nanomaterials*, 10(11), 2208. doi:10.3390/nano10112208
22. Su, J., Ye, S., Yi, X., Lu, F. Q., Yang, X. B., & Zhang, Q. Y. (2017). *Influence of oxygen vacancy on persistent luminescence in ZnGa₂O₄:Cr³⁺ and identification of electron carriers*. *Optical Materials Express*, 7(3), 734. doi:10.1364/ome.7.000734

